JOURNAL OF THERMOPHYSICS AND HEAT TRANSFER
Vol. 6, No. 2, April–June 1992

Diagonal Implicit Scheme for Computing Flows with Finite Rate Chemistry

Scott Eberhardt*
University of Washington, Seattle, Washington 98195
and
Scott Imlay†
Amtec Engineering, Inc., Bellevue, Washington 98004

An algorithm for solving steady, finite rate chemistry, flow problems is presented. The scheme eliminates the expense of inverting the large block matrices that arise when species conservation equations are introduced. This is accomplished by replacing the source Jacobian matrix by a diagonal matrix that is tailored to account for the fastest reactions in the chemical system. A point-implicit procedure is discussed and the algorithm is included into the LU-SGS scheme. Solutions are presented for hypervelocity reentry and hydrogen-oxygen combustion. For the LU-SGS scheme a CFL number in excess of 10,000 has been achieved.

Nomenclature

A = flux Jacobian for ξ-fluxes
$A^{\pm}$ = flux-split Jacobian
A_f = forward Arrhenius rate constant
B = flux Jacobian for η-fluxes
$B^{\pm}$ = flux-split Jacobian
c_{pi} = coefficient of specific heat at constant pressure for species i
D = diagonal matrix for implicit scheme
e_v = vibrational energy
e_v^* = equilibrium vibrational energy
F = convective flux in ξ-direction
F_v = viscous flux in ξ-direction
$\hat{F}$ = TVD flux in the ξ-direction
G = convective flux in η-direction
G_v = viscous flux in η-direction
$\hat{G}$ = TVD flux in the η-direction
H = enthalpy
h = static enthalpy
J = Jacobian of grid transformation
K_{eq} = equilibrium constant
k_b = backward reaction rate
k_f = forward reaction rate
M = Mach number
M_i = molecular weight of species i
n = number of species
p = pressure
Q = vector of conservation variables
R = universal gas constant
RHS = residual (right-hand side) at iteration n
R_i = gas constant of species i
T = gas temperature (translational and rotational)
T_v = vibrational temperature
t = time
U = contravariant velocity in ξ-direction
u = velocity in x-direction
V = contravariant velocity in η-direction
v = velocity in y-direction
W = source term for finite rate chemistry
w_i = finite rate source term for species i
w_{vib} = source term for vibrational relaxation
y_i = mole fraction of species i
Z = Jacobian of source term
$z_{m,n}$ = elements of matrix Z
β = dissipation parameter
β_c = relaxation parameter for chemistry
γ = ratio of specific heats
η = generalized coordinate
η_f = Arrhenius rate coefficient
θ = Arrhenius rate coefficient
μ_i^0 = standard state Gibbs free energy of species i
ν_r = stoichiometric coefficient for reaction r
ξ = generalized coordinate
ρ = density
ρ_i = density of species i
$\rho(Z)$ = spectral radius of matrix Z
$\sigma(Z)$ = matrix with spectral radius of matrix Z on the diagonal
τ_i = characteristic reaction time for species i
ϕ = fuel equivalence ratio

Subscripts and Superscripts

i = index for species
j = index for ξ-direction and species
k = index for η-direction
n = index for iteration count—superscript
n = index for last species—subscript
r = index for reaction
vib = vibration

Introduction

HYPERSONIC flowfields can be expensive to calculate when nonequilibrium flow physics must be included. The expense comes from the need to solve large systems of equations that include the nonequilibrium relaxation equations that arise in addition to the usual mass, momentum, and energy conservation equations. If all chemical species of interest are taken into account, computing three-dimensional flowfields related to Aeroassist Orbital Transfer vehicles, or generic transatmospheric vehicles, may be beyond the capabilities of today's computers.

To model flows with finite rate chemical reactions a continuity equation is carried for each chemical species that oc-

Presented in part as Paper 90-1577 at the AIAA 21st Fluid Dynamics, Plasma Dynamics and Lasers Conference, Seattle, WA, June 18–20, 1990; received Dec. 7, 1990; revision received May 4, 1991; accepted for publication May 24, 1991.

*Assistant Professor, Department of Aeronautics and Astronautics. Member AIAA.
†Senior Engineer. Member AIAA.

curs. Some reaction mechanism models can more than triple the size of the equation set. To make matters worse, there are often disparate chemical time scales among the species continuity equations, requiring more rigorous numerical treatment. Therefore, a method is sought to minimize the amount of computational work required to solve high-speed, chemically reacting flowfields.

One of the first attempts to accommodate the numerical stiffness was presented in a NASA TN by Lomax and Bailey.[1] In that work a simple, steady, one-dimensional problem was solved giving a system of ODEs. The source term, representing the chemical reaction equations were solved implicitly. This leads to a point-implicit numerical scheme where block matrices must be inverted at each point. In a paper by Bussing and Murman[2] the unsteady, multidimensional equations modeling reacting flow were solved. Here, the convection terms were solved explicitly while the chemical source terms were treated implicitly, as in the Lomax report. Again, this leads to a costly point-implicit scheme because matrices are inverted at each point. Although this eliminates the stiffness problem, the cost can be prohibitive for large numbers of species.

Numerous attempts at coupling finite rate chemistry with computational fluid dynamics codes have been successful but expensive. A successful point-implicit procedure has been introduced by Yee and Shinn[3] for hydrogen-air chemistry. Gnoffo et al.[4] and Candler and MacCormack[5] have solved AOTV-like flows with coupled chemistry using implicit algorithms. Dash,[6] Shang and Josyula,[7] and Widhopf and Wang,[8] to name a few, have concentrated on hypersonic vehicles with similar success. Many of these simulations are too expensive or too specialized to be of practical use as a design tool.

Another, and rather clever, attempt at coupling finite rate reactions to fluid calculations was done by Park and Yoon.[9] Their method combines the approximate Jacobian method of the LU-SGS algorithm of Yoon and Jameson[10] with a simplified Park chemical model without ionization. The result is that only 3×3 matrices must be inverted. Unfortunately, their code is not general in that as more species are added (ionized species, etc.) the block matrices grow. Their results, however, do represent a breakthrough because converged solutions are obtained on 32×32 grids within three CPU minutes on a Cray Y-MP.

In this paper we present an algorithm that uses the LU-SGS scheme combined with a diagonal algorithm for finite rate chemistry. The advantage of this approach is that no matrix inversions are required. First, we describe the diagonal method in a point-implicit format to illustrate the procedure. Solutions to the self-similar, conical Euler equations are shown with comparisons to the Bussing/Murman procedure.

A description of the LU-SGS scheme is then presented followed by a series of solutions for a variety of hypervelocity conditions with several accepted reaction models. These solutions are compared against each other and experiments where applicable.

Finite Rate Equations

Coupling finite rate chemistry and thermal nonequilibrium into a computational fluid dynamics code can be accomplished by replacing the global continuity equation with a set of chemical species equations and by adding a vibrational energy equation. The full, two-dimensional Navier-Stokes equations in generalized curvilinear coordinates can be written in a compact vector form given by

$$\frac{\partial \boldsymbol{Q}}{\partial t} + \frac{\partial \boldsymbol{F}}{\partial \xi} + \frac{\partial \boldsymbol{G}}{\partial \eta} + \frac{\partial \boldsymbol{F}_v}{\partial \xi} + \frac{\partial \boldsymbol{G}_v}{\partial \eta} = \boldsymbol{W} \tag{1}$$

where Q are the conservation variables, F and G are the convective fluxes, F_v and G_v are the viscous fluxes, and W are the production and reduction rates for the nonequilibrium processes. The vectors $\boldsymbol{Q}$, $\boldsymbol{F}$, and $\boldsymbol{W}$ are written here for illustration. A complete description of the other terms can be found in Refs. 5 and 11.

$$\boldsymbol{Q} = J^{-1}\begin{bmatrix} \rho_1 \\ \rho_2 \\ \vdots \\ \rho_n \\ \rho_u \\ \rho_v \\ e \\ e_v \end{bmatrix}, \quad \boldsymbol{F} = J^{-1}\begin{bmatrix} \rho_1 U \\ \rho_2 U \\ \vdots \\ \rho_n U \\ \rho u U + \xi_x p \\ \rho v U + \xi_y p \\ U(e + p) \\ U e_v \end{bmatrix} \tag{2}$$

$$\boldsymbol{W} = J^{-1}\begin{bmatrix} w_1 \\ w_2 \\ \vdots \\ w_n \\ 0 \\ 0 \\ 0 \\ w_{\text{vib}} \end{bmatrix} \tag{3}$$

The first n rows of the equation correspond to the species conservation laws. It is the expansion of the global mass conservation law into n species conservation laws that gives rise to a significant increase in computational effort and is the motivation for the numerical scheme proposed here. The two following rows, $n + 1$ and $n + 2$, correspond to the x- and y-momentum conservation laws, respectfully. The second to last equation expresses total energy conservation. In some calculations we have included the last equation, a vibrational energy conservation equation, to simulate thermal nonequilibrium. In the equations u and v are the two Cartesian velocities, ρ_i are the species densities, ρ is the global density, i.e.

$$\rho = \sum_{i=1}^{n} \rho_i$$

e is the total energy per unit volume and e_v is the vibrational energy per unit volume. The terms w_i represent the production or reduction of a species due to chemical reactions; w_{vib} is the vibrational energy relaxation forcing function.

A generalized curvilinear coordinate system is used giving rise to a grid Jacobian J given by

$$J^{-1} = x_\xi y_\eta - y_\xi x_\eta \tag{4}$$

and contravariant velocities U and V

$$\begin{aligned} U &= \xi_x u + \xi_y v \\ V &= \eta_x u + \eta_y v \end{aligned} \tag{5}$$

The system of equations is closed by introducing an equation of state for pressure p. Here, we make use of Dalton's law so pressure is given by

$$p = \sum_{i=1}^{n} \frac{\rho_i}{M_i} RT \tag{6}$$

where M_i is the molecular weight of the ith species, and R is the universal gas constant. The static temperature of the mixture T is backed out from the definition of total energy

$$\sum_{i=1}^{n} \frac{\rho_i}{\rho}\left(\bar{c}_{p_i} - \frac{R}{M_i}\right) T = \frac{e}{\rho} - \frac{1}{2}(u^2 + v^2) \tag{7}$$

where $\bar{c}_p$, is H/R_iT and is obtained as a function of temperature from the JANAF tables[12] or the polynomial fits by Esch et al.[13]

Details of the viscous terms are not presented here in the interest of brevity, although a procedure similar to that used by Candler and MacCormack[5] is used for the air-dissociation calculations. The vibrational relaxation scheme is a simple Landau-Teller model.

Source terms for species production and reduction are presented in the Appendix.

The goal of the algorithm is to make calculations of flows in thermochemical nonequilibrium more efficient, given the limitations of today's computers. The algorithm has been applied to one-, two-, and three-dimensional inviscid and viscous flows. The details of the physical modeling are not important to understanding the diagonal algorithm, so no attempt is made to justify or discuss the details of the particular models we use.

Point-Implicit Procedure

The diagonal algorithm is an approximate Newton method with a diagonalized source Jacobian matrix. First, in this section, the method is described for a point-implicit scheme. In a later section, a fully implicit algorithm is described. In the point-implicit method the chemical source terms are solved implicitly, whereas the convective fluxes are solved explicitly using Roe's first-order scheme,[14] the Harten-Yee second-order TVD scheme,[15] or the Steger-Warming scheme.[16] In addition, the scheme has been applied to the Yee and Shinn, TVD-MacCormack, point-implicit scheme.[3]

For illustration we will use finite difference terminology, although the implicit procedure has been introduced into both finite difference and finite volume codes. An explicit scheme, in one-dimension, can be written

$$\Delta Q = Q_j^{n+1} - Q_j^n = -\Delta t \left[\frac{\tilde{F}_{j+1/2}^n - \tilde{F}_{j-1/2}^n}{\Delta x} - W_j^n \right] \quad (8)$$

where $\tilde{F}$ are the fluxes defined by the finite difference algorithm.

The numerical method presented here does not alter the explicit part of the algorithm so it will be denoted by *RHS*, i.e

$$RHS^n = \frac{\tilde{F}_{j+1/2}^n - \tilde{F}_{j-1/2}^n}{\Delta x} - W_j^n \quad (9)$$

The point-implicit approach is introduced to solve the source term implicitly, i.e.:

$$\Delta Q = -\Delta t \left[\frac{\tilde{F}_{j+1/2}^n - \tilde{F}_{j-1/2}^n}{\Delta x} - W_j^{n+1} \right] \quad (10)$$

Following a simple linearization of the source term, i.e

$$W_j^{n+1} = W_j^n + Z_j^n \Delta Q + \mathcal{O}(\Delta Q^2) \quad (11)$$

where Z is the Jacobian matrix of the source term W, ($Z = \partial W/\partial Q$, and is given in the Appendix) we can write a point-implicit algorithm

$$[I - \Delta t Z_j^n]\Delta Q = -\Delta t RHS^n \quad (12)$$

This method, used by Bussing and Murman,[2] eliminates the stiffness problem and allows the solution to be updated with a Δt dictated by the CFL condition. The difficulty comes when the number of species is large because inverting $[I - \Delta t Z_j^n]$ becomes expensive. The technique outlined here approximates this matrix by a diagonal matrix for which no inversion is required. The elements of the new diagonal matrix represent the rate of production, or reduction, of a particular species from its fastest reaction. An explanation of this step will become clearer in the following discussion.

Upon examination of the elements of Z and $z_{m,n}$, it is found that each is proportional to the reaction times of all reactions in which both species m and n participate. If we take the limiting case of one fast reaction, involving species m and n, compared to many slow reactions, then $z_{m,n}$ can be approximated by the one fast reaction. The essence of the standard point-implicit algorithm is that the matrix preconditioner scales the chemical time steps to accommodate these fast reactions. Our intention is to replace Z by a diagonal matrix with the spectral radius of Z along the diagonal, i.e.

$$[1 + \Delta t \rho(Z_j^n)]\Delta Q = -\Delta t RHS^n \quad (13)$$

to achieve the same goal. For our example of the limiting case, this makes the new matrix proportional to the fastest reaction rate. Of course, this amounts to nothing more than rescaling Δt so the scheme will be explicitly stable. In effect, the scheme underrelaxes the chemical source term.

Finding the eigenvalues, and, thus, the spectral radius for Z exactly can be difficult, so rather than using the spectral radius, we choose to use the 2-norm of Z. This gives a conservative estimate for the spectral radius $\rho(Z)$.

Returning to the example of the limiting case of one fast reaction and many slow reactions it is found that all reactions, fast and slow, are underrelaxed with this procedure, thus, slowing down convergence. Some species may only be involved in slow reactions and do not need to be underrelaxed. Therefore, the diagonal elements are instead found by computing the 2-norm of the elements $z_{m,n}$ along each row, separately. Thus, each of the species, and the momentum and energy equations, are relaxed at appropriate time steps. Species that are only catalysts, or are inert are then updated with a time scale suitable for the fluid. We write our point-implicit algorithm as follows:

$$\left[I + \text{DIAG}\left(\frac{\Delta t}{\tau_i} \right) \right] \Delta Q = -\Delta t RHS^n \quad (14)$$

where τ_i is the characteristic time for the production, or reduction, of species i and is found from the 2-norm of row i of matrix Z.

The method is simple and is easy to program because the information required to compute τ_i is all contained in the calculation for w_i, the explicit source term, which is shown in the Appendix. The approximation made does not affect the steady-state solution because the residual operator *RHS* goes to zero and the implicit operator is irrelevant. Also, it is independent of the particular algorithm used to calculate *RHS*. The primary disadvantage is that the scheme is unsuitable for time-dependent problems.

One other "trick" that is used is to recognize that any time scale shorter than the time a fluid particle travels one cell can be considered to be a subgrid time scale. These subgrid time scales cannot and need not be resolved. Therefore, we can artificially reset the Damköhler number such that a fast reaction reaches equilibrium in one cell and not in, say, 1/1000 of a cell. A Damköhler number of one will allow the reaction to reach approximately 1/e of the final state. We use a Damköhler number of ten. Lower values will smear the shock slightly for equilibrium reactions. Such a procedure serves the same purpose as using an average temperature such as recommended by Oran and Boris.[17] Note that this procedure must be used for both the diagonal and the full Jacobian, point-implicit algorithms, so it is not unique to the method.

Point-Implicit Method Results

To illustrate the point-implicit method we start with the conical flow equations. This self-similar problem is useful for solving steady, high Mach number flows in one dimension. In this example a five-species, 21-reaction model of Wray[18] is used. Note that an independent reaction is considered for

each collision partner in a dissociation reaction. For comparison, the block-inversion method has also been tested. Note that for the block-inversion method a full 8 × 8 matrix is inverted.

Converged solutions for the diagonal algorithm and the full block-inversion algorithm are identical. Figure 1 is a plot of a radial line away from a cone at 54 deg in a Mach 20 flow for the diagonal algorithm (results for the full block-inversion algorithm are not shown because the results are identical). The freestream pressure is 100 N/m^2 and the temperature is 270 K. The computation required for the diagonal algorithm was almost a full order-of-magnitude less than the full Jacobian, point-implicit method. Simulations were run with Courant numbers approaching the explicit limit for the flux terms; i.e., 0.8. These solutions are on a coarse, 18-point mesh. Note that the residual operator, the two-norm of the right-hand side, is identical for both cases so the converged solutions should be identical.

Figure 2 is the convergence history comparing the CPU time needed for the diagonal algorithm versus the block-inversion method. These times are CPU seconds on a DecStation 2100. Note that this is the only comparison of work between the diagonal algorithm and the block-inversion method because the block-inversion method becomes too expensive for multidimensional calculations on the DecStation 2100.

Experience with the point-implicit diagonal scheme indicates that it works with any choice of algorithm for the convective fluxes and that it is more robust than the block-inversion approach. This latter result at first came as a surprise but it is believed that the diagonal method underrelaxes the source term so it is more forgiving of the strong nonlinearities inherent in reacting flows. It is again stressed that the steady-state solution will be dependent on the right-hand side and the modeling used there. The diagonal method only speeds the relaxation to steady state.

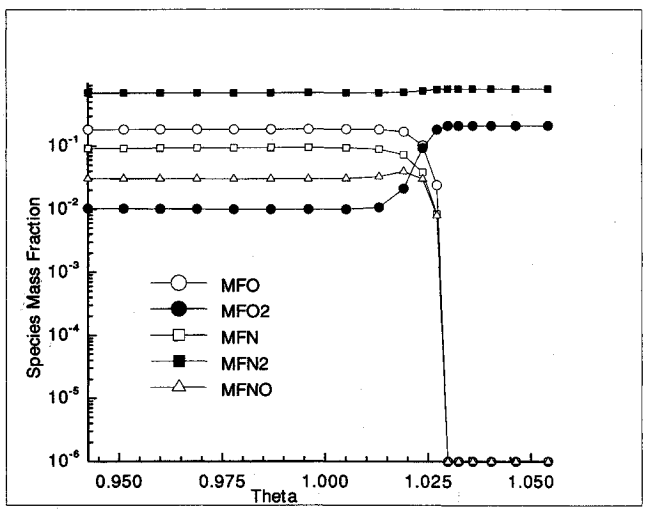

Fig. 1 Species mass fraction from diagonal point-implicit method.

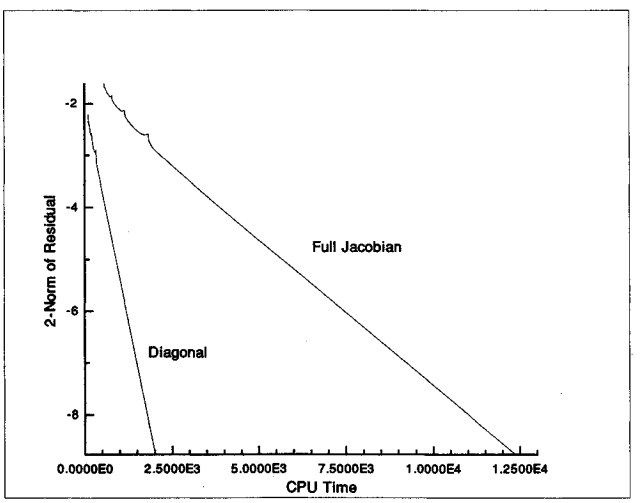

Fig. 2 Residual history vs CPU time on a DecStation 2100.

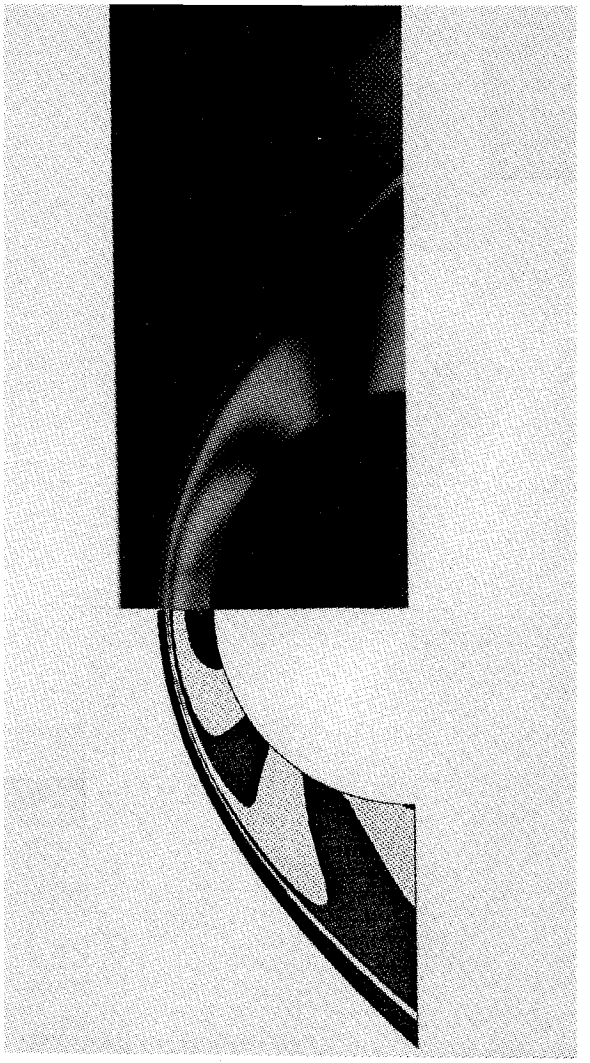

Fig. 3 Cylinder in N_2/N, Mach 6.13 flow: top—from Hornung[20]; bottom—from diagonal LU-SGS calculation.

LU-SGS Method

The addition of the diagonal method for finite rate chemistry is ideally suited to the LU-SGS scheme of Yoon and Jameson.[10] A review of Yoon's and Jameson's algorithm for two-dimensional calculations will demonstrate the motivation for combining the finite rate chemistry with LU-SGS. Yoon and Jameson define a flux splitting based on the spectral radius of the flux-Jacobians, i.e. define

$$A^{\pm} = \tfrac{1}{2}[a \pm \beta\sigma(A)], \quad B^{\pm} = \tfrac{1}{2}[B \pm \beta\sigma(B)] \qquad (15)$$

where A is the flux-Jacobian of F ($A = \partial F/\partial Q$), and B is the flux-Jacobian of G. $\sigma(A)$ is an identity matrix with the spectral radius of A on the diagonal. β is a dissipation parameter whose value is typically selected between 1.5 and 2.

A first-order, implicit, upwind differencing scheme can be written

$$[I + \Delta t(A^-_{j+1,k} + A^+_{j,k} - A^+_{j-1,k}) + \Delta t(B^-_{j,k+1} - B^-_{j,k} + B^+_{j,k} - B^+_{j,k-1})]\Delta Q = RHS \qquad (16)$$

Table 1 Summary of LU-SGS simulations

Run	Mach #	Reaction model	Grid size	Algorithm
1	6.13	N_2–N	22 × 22	Steger-Warming
2	6.13	N_2–N	34 × 34	Steger-Warming
3	6.13	N_2–N	50 × 50	Steger-Warming
4	6.13	N_2–N	22 × 22	Roe
5	6.13	N_2–N	34 × 34	Roe
6	6.13	N_2–N	50 × 50	Roe
7	6.13	Wray	22 × 22	Steger-Warming
8	6.13	Park	22 × 22	Steger-Warming

Table 2 CPU time summary

Run	Total iterations	CPU time	L_2 drop	CPU—10^{-6}	Iterations—10^{-6}
1	3000	190	11.55	116	1730
2	3000	347	6.69	329	2710
3	5000	1048	8.21	770	3675
4	3000	171	12.30	84	1465
5	3000	313	7.24	253	2425
6	5000	981	7.88	692	3715
7	3000	370	10.77	230	1865
8	9400	1501	6.00	1501	9400

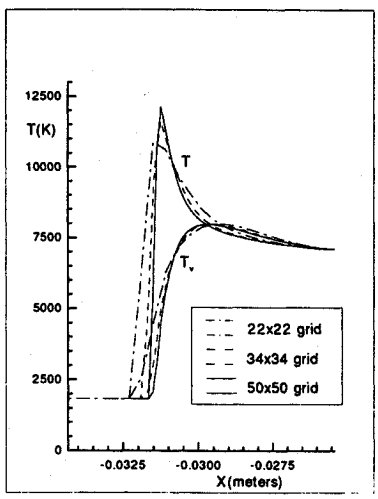

Fig. 4a Grid sensitivity study for Hornung case using Steger-Warming fluxes in diagonal LU-SGS scheme—temperature.

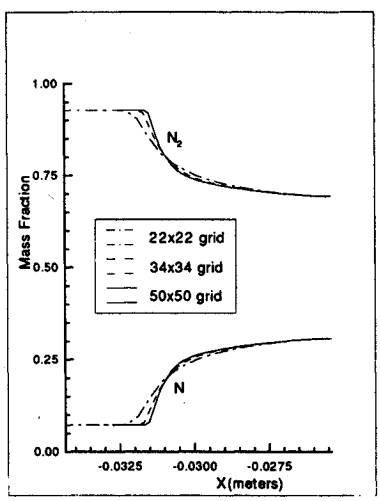

Fig. 4b Grid sensitivity study for Hornung case using Steger-Warming fluxes in diagonal LU-SGS scheme—N–N_2 concentrations.

Just as in the case of the point-implicit method discussed earlier, this implicit procedure can be applied to any explicit procedure on the right-hand side. The trick is that the terms $(-A^-_{j,k} + A^+_{j,k})$ and $(-B^-_{j,k} + B^+_{j,k})$ give $\beta\sigma(A)$ and $\beta\sigma(B)$, respectively. Thus, the algorithm can be rewritten

$$[(I + \Delta t(\sigma(A) + \sigma(B)))$$
$$+ \Delta t(A^-_{j+1,k} - A^+_{j-1,k} + B^-_{j,k+1} - B^+_{j,k-1})]\Delta Q$$
$$= RHS \tag{17}$$

In this form a lower-upper decomposition of the operator is simple and the result is

$$[D - \Delta t(A^-_{j-1,k} + B^-_{j,k-1})]D^{-1}$$
$$[D + \Delta t(A^+_{j+1,k} + B^+_{j,k+1})]\Delta Q = RHS$$

where

$$D = I + \Delta t(\sigma(A) + \sigma(B)) \tag{18}$$

The algorithm is stable as $\Delta t \to \infty$ and involves no block matrix inversions. For a two-dimensional, ideal-gas calculation we have found that the additional CPU time required to run LU-SGS is only about 10% greater than the time required to run our explicit, second-order Harten-Yee scheme per iteration. With the implicit time-stepping, however, converged solutions can be obtained in far fewer iterations.

If we now include finite-rate chemistry into the LU-SGS procedure the steps taken are the same except that the diagonal element D changes to reflect the source Jacobian Z. The matrix D is given as

$$D = I + \Delta t(\sigma(A) + \sigma(B)) - \Delta t Z \tag{19}$$

and is no longer diagonal because Z is a block matrix. The advantage of the LU-SGS scheme has been lost. The diagonalization procedure described in the previous section for the point-implicit method is easily adapted to the LU-SGS scheme. We replace Z by its equivalent diagonal matrix, i.e.

$$D = I + \Delta t(\sigma(A) + \sigma(B)) + \text{DIAG}\left(\frac{\Delta t}{\tau_i}\right) \tag{20}$$

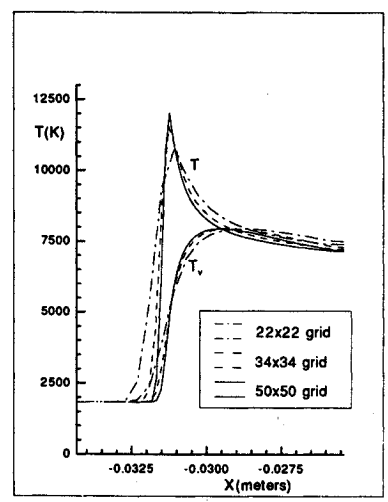

Fig. 5 Hornung case using Roe's flux-splitting in diagonal LU-SGS scheme.

which again leaves us with no block matrices to invert.

The greatest savings will be achieved when large systems of equations are used; such as for the Park reaction model[19] will 11 species and a vibrational energy equation. Without the diagonal method, 12 × 12 matrices would have to be inverted.

LU-SGS Results

A series of calculations have been performed for hypervelocity, nonequilibrium flows. A three-dimensional code, HANA, has been produced that uses the LU-SGS relaxation procedure in conjunction with a Steger-Warming, Roe, or Harten-Yee scheme. The code allows reaction models and species to be specified from an input file. Thermal-nonequilibrium and a $\kappa - \epsilon$ turbulence model are included. (Note that the diagonal procedure has also been applied to the $\kappa - \epsilon$ turbulence model to retain a diagonal system.) Because HANA is a full three-dimensional code, two-dimensional and axisymmetry are attained by solving a three-dimensional slice five grid cells wide. This will manifest itself in more moderate performance in terms of CPU time. The following results are obtained using HANA on a Cray X-MP.

The first series of results are for code validation. They represent a cylinder in a Mach 6.13 flow of pure nitrogen at a freestream temperature of 1833 K. The experimental work of Hornung[20] is used to validate the results. Figure 3 is a comparison of our calculation with the experiment. The agreement of the shock location between the experiment and numerical simulation demonstrates that the nonequilibrium chemical and thermodynamic models are correct for this application and that the diagonal algorithm correctly converges to the proper solution. The runs and reaction models presented for this application are summarized in Table 1 and the flow is assumed to be inviscid.

A grid resolution study shows that the code converges well and the details around the shock wave become more refined as the grid is refined. Figure 4a is a plot of temperature and vibrational temperature along the stagnation line for three grid resolutions, 22 × 22, 34 × 34, and 50 × 50 using the Steger-Warming algorithm (runs 1–3). Figure 4b shows N and N_2 concentrations.

The 22 × 22, 34 × 34, and 50 × 50 calculations have been run using Roe's scheme and stagnation line temperatures are shown in Fig. 5 for comparison.

To illustrate the effects of the number of species on the computational costs the same calculation, with a 22 × 22 grid, was run using Wray's species and Park's 11 species model but with only N_2 and N present in the freestream. The CPU time for these runs are recorded in Table 2. The CPU time listed in column 3 is the total time in seconds taken to reach the number of iterations in column 2. The corresponding drop in the two-norm of the residual operator is listed in column 4. Columns 5 and 6 are the CPU time and number of iterations taken to reach a 6-order-of-magnitude drop in the two-norm, respectively.

Recall that the code is fully three-dimensional, so the two-dimensional calculations actually use five cells across to achieve a single plane of data. An optimized two-dimensional calculation would be significantly cheaper to run.

Two additional validation calculations are shown that compare solutions generated with HANA to experimental results. These two comparisons test larger, more complex reaction models than the previous calculations. The first is a comparison of the computed and experimental shock detachment distance from the flow about a sphere in hypervelocity air. The experiment is from Lobb.[21] Both a two-temperature Wray model and Park model were used for the calculation. Because ionization is negligible, both solutions are effectively identical and in excellent agreement with the experiment. Figure 6 shows the computed shock location, which lies on the three data points obtained from the Lobb experiment. The second validation shows a comparison of the computed shock detachment distance to a sphere fired in a combustible mixture of hydrogen/oxygen and hydrogen/air. The experimental data are from Lehr.[22] Figures 7a and 7b again show the excellent agreement obtained from the computations.

Finally, a three-dimensional calculation is performed for conditions selected to model the AFE (Aeroassist Flight Experiment). The flow is at Mach 33 and the freestream density and pressure simulate an altitude of 75,155 meters. The calculation uses the two-temperature Park model. Translational temperature, vibrational temperature, diatomic oxygen, and

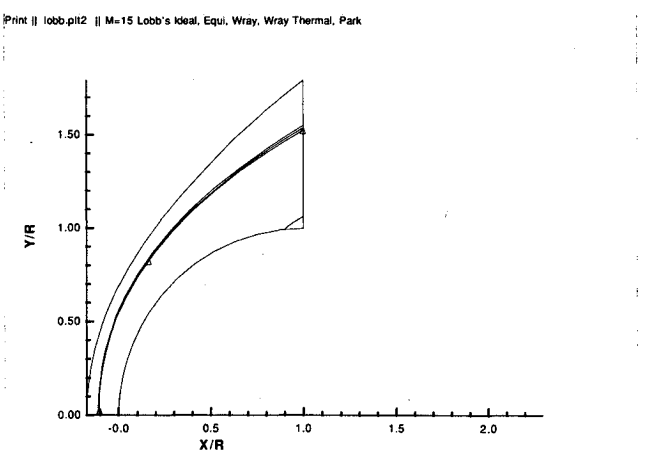

Fig. 6 Predicted shock location for Mach 15 flow about a sphere compared to the experiment of Lobb.

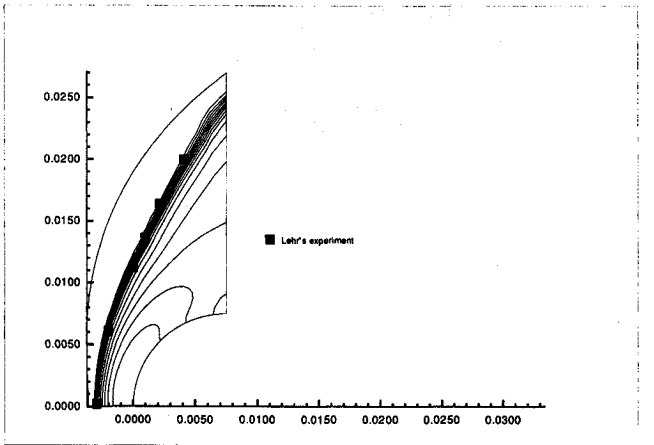

Fig. 7a Predicted shock location of a sphere in H_2/O_2 mixture compared to the experiment of Lehr.

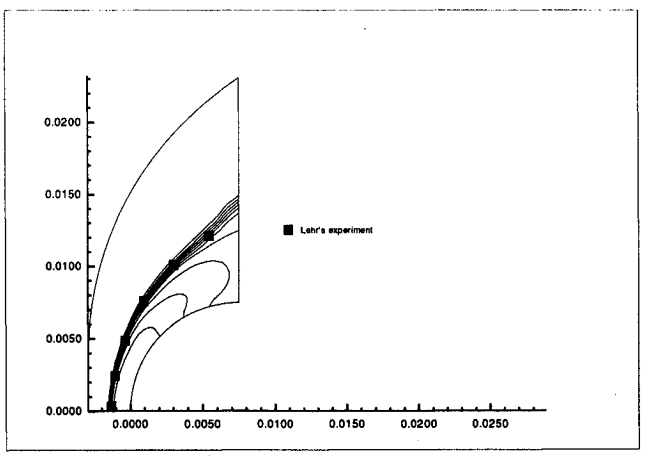

Fig. 7b Predicted shock location of a sphere in H_2/air mixture compared to the experiment of Lehr.

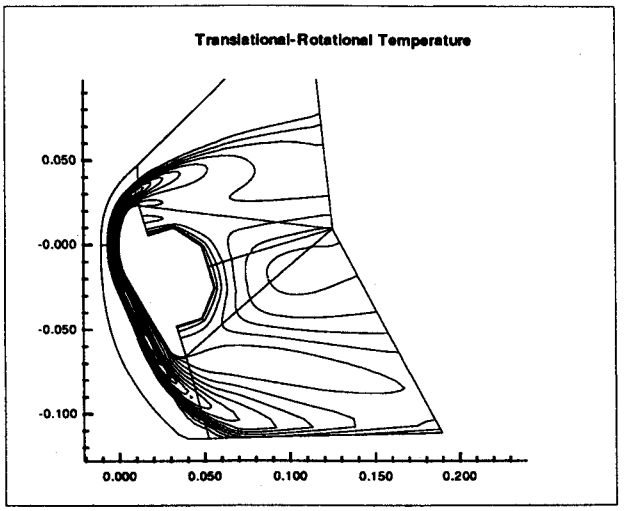

Fig. 8a Translational temperature contours along symmetry plane for Mach 33, AOTV using Park model.

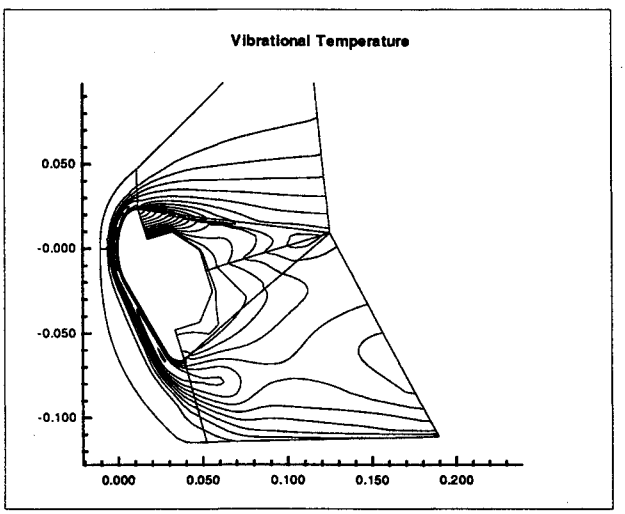

Fig. 8b Vibrational temperature contours along symmetry plane for Mach 33, AOTV using Park model.

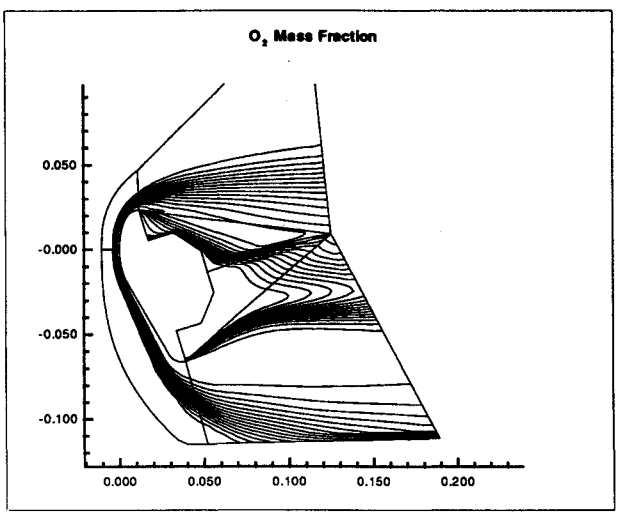

Fig. 8c O_2 mass fraction contours along symmetry plane for Mach 33, AOTV using Park model.

electron mass fraction contours are shown in Figs. 8a–8d, respectively. Figure 9 is a plot of species mass fractions along the stagnation line for both the Park model and the Wray model. The grid used in these calculations uses 167,000 points

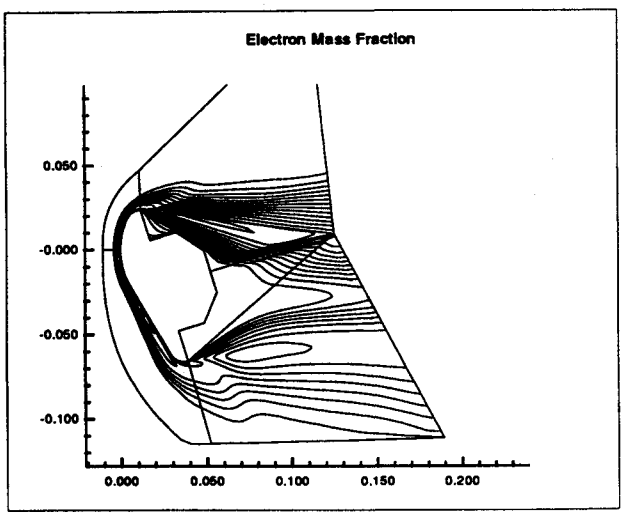

Fig. 8d Electron mass fraction contours along symmetry plane for Mach 33, AOTV using Park model.

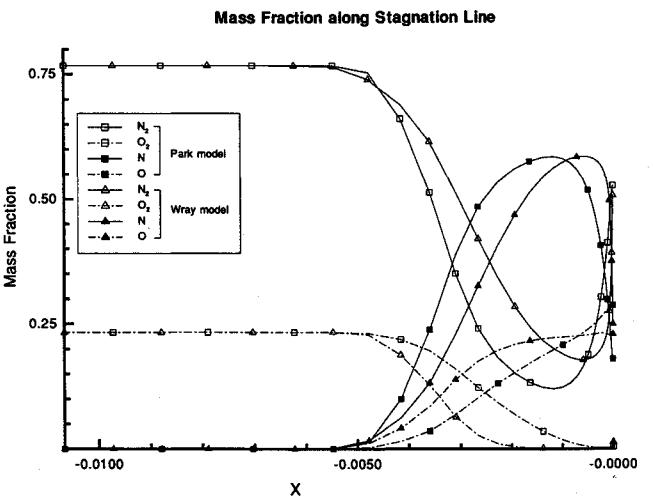

Fig. 9 Species mass fractions along stagnation streamline for Mach 33, AOTV using Park and Wray model.

and a converged solution took 26 hours on a Cray Y-MP for the Park model.

In some cases a CFL number of 10,000 has been reached. Generally, the solution procedure must start at a more moderate CFL number to ease the transient behavior. However, the CFL number is quickly ramped up to large values without a loss in stability.

Conclusions

An approximate Newton method is introduced for solving reacting flows. The algorithm eliminates the stiffness problem associated with finite rate chemistry without adding the extra cost of inverting large matrices. The algorithm has seen extensive use on a variety of reacting flow problems with a selection of explicit flux algorithms and reaction models. The method is robust and achieves the goal of making three-dimensional, reacting flow calculations possible.

Appendix

The species production term due to chemical reactions is found using an Arrhenius rate equation for the forward reaction. The reverse reaction rate is obtained by making use of the equilibrium condition. The production rate terms w_n

are given as

$$w_n = M_n \sum_r (\nu_r^f - \nu_r^b) \left[\kappa_f \prod_i y_i^{\nu_i^f} - k_b \prod_i y_i^{\nu_i^b} \right] \quad \text{(A1)}$$

where the index r refers to a specific reaction, the index i refers to a specific species, whose mole fraction is given by y_i, and k_f is the forward rate constant given by

$$k_f = A_f T^{\eta_f} e^{\frac{-\theta}{T}} \quad \text{(A2)}$$

A_f, η_f, and θ are the three Arrhenius coefficients. T is the temperature. Note that for Park's two-temperature model, T is taken to be $\sqrt{TT_{\text{vib}}}$ to account for thermal nonequilibrium effects of the flow. The reverse reaction rate k_b is found by

$$k_b = \frac{k_f}{K_{\text{eq}}}$$

and K_{eq} is

$$K_{\text{eq}} = \frac{e - \sum_i \nu_i \hat{\mu}_i^0 / R_i T}{(R_n T) \sum_i \nu_i} \quad \text{(A3)}$$

In the above equations, ν are the stoichiometric coefficients for the reactions. μ_i^0 is the standard state Gibb's free energy of species i.

The Jacobian term can be computed analytically or numerically. The analytical expression for the terms involving the species equations only gives

$$z_{m,n} = \frac{\partial w_m}{\partial \rho_n} = \sum_r (\nu_r^f - \nu_i^b)_m \left[\frac{\nu_n^f}{y_n} k_f \prod_i y_i^{\nu_i^f} - \frac{\nu_n^b}{y_n} k_b \prod_i y_i^{\nu_i^b} + \prod_i y_i^{\nu_i^f} \frac{\partial k_f}{\partial y_n} - \prod_i y_i^{\nu_i^b} \frac{\partial k_b}{\partial y_n} \right] \quad \text{(A4)}$$

For the diagonal approach we have made the assumption that the terms involving $\partial k_f / \partial y_n$ and $\partial k_b / \partial y_n$ are unimportant and so have been neglected.

If only the species terms are involved the normal point-implicit procedure would involve the inversion of the following matrix:

$$Z = \frac{\partial W}{\partial Q} = \begin{bmatrix} \frac{\partial w_1}{\partial \rho_1} & \frac{\partial w_1}{\partial \rho_2} & \cdots & \frac{\partial w_1}{\partial \rho_{n-1}} & \frac{\partial w_1}{\partial \rho_n} \\ \frac{\partial w_2}{\partial \rho_1} & \frac{\partial w_2}{\partial \rho_2} & \cdots & \frac{\partial w_2}{\partial \rho_{n-1}} & \frac{\partial w_2}{\partial \rho_n} \\ \frac{\partial w_3}{\partial \rho_1} & \frac{\partial w_3}{\partial \rho_2} & \cdots & \frac{\partial w_3}{\partial \rho_{n-1}} & \frac{\partial w_3}{\partial \rho_n} \\ \vdots & \vdots & \cdots & \vdots & \vdots \end{bmatrix} \quad \text{(A5)}$$

In the diagonal method this matrix is replaced by

$$\hat{Z} = \begin{bmatrix} \frac{1}{\tau_1} & 0 & 0 & \cdots & 0 \\ 0 & \frac{1}{\tau_2} & 0 & \cdots & 0 \\ 0 & 0 & \frac{1}{\tau_3} & \cdots & 0 \\ 0 & 0 & 0 & \cdots & \frac{1}{\tau_n} \end{bmatrix} \quad \text{(A6)}$$

where

$$\frac{1}{\tau_m} = \beta_c \left[\sum_n \left(\frac{\partial w_m}{\partial \rho_n} \right)^2 \right]^{1/2} \quad \text{(A7)}$$

and β_c is a relaxation parameter greater than one.

Acknowledgments

This work was supported by NASA Marshall Space Center, Contract NAS8-37406 and by the National Science Foundation through a Presidential Young Investigator Award.

References

[1]Lomax, H., and Bailey, H. E., "A Critical Analysis of Various Numerical Integration Methods for Computing the Flow of a Gas in Chemical Nonequilibrium," NASA TN D-4109, Aug. 1967.

[2]Bussing, T. R. A., and E. M. Murman, "A Finite Volume Method for the Calculation of Compressible Chemically Reacting Flows," AIAA Paper 85-0331, Twenty-third Aerospace Sciences Meeting, Reno, NV, Jan. 1985.

[3]Yee, H. C., and Shinn, J. L., "Semi-Implicit and Fully-Implicit Shock Capturing Methods for Hyperbolic Conservation Laws with Stiff Source Terms," NASA TM 89415, Dec. 1986.

[4]Gnoffo, P. A., McCandless, R. S., and Yee, H. C., "Enhancements to Program Laura for Computation of Three-Dimensional Hypersonic Flow," AIAA Paper 87-0280, Twenty-fifth Aerospace Sciences Meeting, Reno, NV, Jan. 1987.

[5]Candler, G., and MacCormack, R. W., "The Computation of Hypersonic Ionized Flows in Chemical and Thermal Nonequilibrium," AIAA Paper 88-0511, Twenty-Sixth Aerospace Sciences Meeting, Reno, NV, Jan. 1988.

[6]Dash, S. M., "Recent Advances in Parabolized and Full Navier-Stokes Solvers for Analyzing Hypersonic, Chemically-Reacting Flowfield Problems," AIAA Paper 89-1698, Twenty-fourth Thermophysics Conf., Buffalo, NY, June 1989.

[7]Shank, J. S., and Josyula, E., "Numerical Simulations of Non-Equilibrium Hypersonic Flow Past Blunt Bodies," AIAA Paper 88-0512, Twenty-sixth Aerospace Sciences Meeting, Reno, NV, Jan. 1988.

[8]Widhopf, G. F., and Wang, J. C. T., "A TVD Finite-Volume Technique for Nonequilibrium Chemically Reacting Flows," AIAA Paper 88-2711, Thermophysics, Plasmadynamics and Lasers Conf., San Antonio, TX, June, 1988.

[9]Park, C., and Yoon, S., "A Fully Coupled Implicit Method for Thermo-Chemical Nonequilibrium Air at Sub-Orbital Speeds," AIAA Paper 87-1974, Ninth Computational Fluid Dynamics Conf., Buffalo, NY, June 1989.

[10]Yoon, S., and Jameson, A., "Lower-Upper Symmetric-Gauss-Seidel Method of the Euler and Navier-Stokes Equations," *AIAA Journal*, Vol. 26, No. 9, 1988.

[11]Chuck, C., "Numerical Simulation of Oblique Detonation and Shock Deflagration Waves with a Laminar Boundary-Layer," Ph.D. Dissertation, Univ. of Washington, Dept. of Aeronautics and Astronautics, June, 1990.

[12]Stull, D. R., and Prophet, H., "JANAF" Thermochemical Tables, 2nd ed.," NSRDS-Report 37, National Bureau of Standards, June 1971.

[13]Esch, D. D., Siripong, A., and Pike, R. W., "A Technical Report on Thermodynamic Properties in Polynomial Form For Carbon, Hydrogen, Nitrogen and Oxygen Systems From 300 to 15000K," NASA-RFL-TR-70-3, Nov. 1970.

[14]Roe, P. L., "The Use of the Riemann Problem in Finite Difference Schemes," *Proceedings of the Seventh International Conference on Numerical Methods in Fluid Dynamics, Lecture Notes in Physics*, Vol. 141, 1981.

[15]Yee, H. C., Warming, R. H., and Harten, A., "Implicit Total Variation Diminishing (TVD) Schemes for Steady State Calculations," *Journal of Computational Physics*, Vol. 57, No. 3, 1985.

[16]Steger, J. L., and Warming, R. H., "Flux Vector Splitting of the Inviscid Gasdynamics Equations with Application to Finite-Difference Methods," *Journal of Computational Physics*, Vol. 40, No. 2, 1981, pp. 263–293.

[17]Oran, E., and Boris, J., *Numerical Simulation of Reactive Flow*, Elsevier, New York, 1987.

[18]Wray, K. L., "Chemical Kinetics of High Temperature Air," American Rocket Society International Hypersonics Conf., Aug. 1961.

[19]Park, C., "A Review of Reaction Rates in High Temperature Air," AIAA Paper 89-1740, Twenty-fourth Thermophysics Conf., Buffalo, NY, June, 1989.

[20]Hornung, H., "Nonequilibrium Dissociating Nitrogen Flow over Spheres and Circular Cylinders," *Journal of Fluid Mechanics*, Vol. 53, Part 1, 1972, pp. 149–176.

[21]Lobb, R. K., "Experimental Measurement of Shock Detachment Distance on Spheres Fired in Air at Hypervelocities," *High Temperature Aspects of Hypersonic Flow*, edited by W. C. Nelson, Pergammon, New York, 1964.

[22]Lehr, H. F., "Experiments on Shock-Induced Combustion," *Acta Astronautica*, Vol. 17, 1972, pp. 589–597.